JMEPEG (2017) 26:644–652
DOI: 10.1007/s11665-016-2498-1

1059-9495/$19.00

Experimental Study on Creep Characterization and Lifetime Estimation of RPV Material at 723-1023 K

Lin-Jun Xie, Dong Ning, and Yi-zhong Yang

(Submitted August 31, 2015; in revised form August 1, 2016; published online January 9, 2017)

During the plant operation, nuclear reactor pressure vessel (RPV) is the most critical pressure boundary component for integrity and safety in a light-water reactor. In this paper, the creep behavior and properties for RPV metallic material are studied by conducting constant-temperature and constant-load creep tests at 723, 823, 923 and 1023 K. The θ projection constitutive model was established based on a creep method to describe the high-temperature creep behavior of RPV material. The material parameter θ would be obtained based on experimental data by depending on numerical optimization techniques. The relationship between and among θ, T and σ was evaluated, and the coefficients a_i, b_i, c_i and d_i were obtained. Based on the short-term tests at a high temperature, the values for long-term creep data could be predicted in accordance with parameter θ. Moreover, rupture life, the minimum creep rate and the time reaching to an arbitrary strain can be calculated and may be used to evaluate the damage behavior and properties, so as to be used as a reference for design and safety assessment.

Keywords creep behavior, creep life prediction, data fitting, RPV material, θ projection model

1. Introduction

For the nuclear power plant, retaining the core melts in the RPV, i.e., in-vessel retention (IVR), through the outside water-cooling system of the reactor pressure vessel (RPV) is an important management action after a serious accident. High-temperature creep will occur in the lower sealing connector of RPV for high temperature (773-1473 K) and marked temperature strain in the IVR process. Meanwhile, creep property of the RPV material will decrease because phase or microstructure transformation will be occurred in this material under such high temperature. The structural integrity of RPV can be maintained through the study on high-temperature creep performance of RPV. It is an important issue that we need consider seriously. On the other hand, as far as integrity and safety are concerned, reactor pressure vessel (RPV), as an engineering part, is the most critical pressure boundary component in a light-water reactor. The design criteria for long-term operation must guarantee that creep deformation should not cause excessive distortion over the planned service life and that creep failure should not occur within such a required operating life (Ref 1). So, the creep constitutive model is developed based on creep data to study the rupture life, minimum creep rate and time reaching to an arbitrary strain, to assess possible damage and to define plant life management.

In recent years, most studies on high-temperature material properties have focused on creep constitutive model (Ref 2-4). Various equations have been developed by researchers (Ref 5-10) in order to describe the creep curves accurately in the last few decades, such as power law, continuum damage and the θ projection concept. Evans and Wilshire (Ref 11, 12) have developed the θ projection concept to analyze the creep data with a view to predicting the short- and long-term creep properties for a variety of metallic materials (Ref 13), such as 2.25Cr-1Mo steels (Ref 14), modified 9Cr-1Mo steel (Ref 15), Al-Cu-Mg alloy (Ref 16), 7075 aluminum alloy (Ref 17),austenitic stainless steel (Fe-Ni-Cr-Al) (Ref 18) and nickel-based Hastelloy-X alloy (Ref 19). Dyson et al. (Ref 20) researched and developed an optimized procedure to calibrate the constitutive parameters of a continuum damage mechanics model for 1/2Cr-1/2Mo-1/4V ferritic steel. Jiang et al. (Ref 21) developed a power law equation to predict the minimum creep strain rates by investigating the properties of Mg-5Li-Al-0.5Ca and Mg-5Li-3Al-1Ca at different temperatures and stresses. Tahami (Ref 22) mentioned that creep constitutive parameters were calculated for Norton power law and Prandtl law, which could be used to estimate creep behavior of structures at different operating conditions.

Experimental studies on creep test are so significant because RPV material is an important RPV material in nuclear power engineering. In this study, a complete three stages of creep curve can be concluded based on the available experimental data of RPV material by using the θ projection method. The main objective is to acquire the creep data, creep constitutive equations, rupture life and the minimum creep rate, so as to predict the time reaching to an arbitrary strain and evaluate the damage behavior and properties of RPV material.

2. *h*-Projection Constitutive Model

Creep is a performance characteristic of the material at high temperatures. It is formed through a long-term process of inelastic deformation accumulation under a constant stress at high temperatures. The θ projection concept has been introduced by

Lin-Jun Xie, College of Mechanical Engineering, Zhejiang University of Technology, Hangzhou 310014, China; and **Dong Ning** and **Yi-zhong Yang**, Shanghai Nuclear Engineering Research & Design Institute, Shanghai 200233, China. Contact e-mail: linjunx@zjut.edu.cn.

Evans and Wilshire (Ref 11) to express a creep curve in 1985. This physical model contains the strain hardening, precipitation and accumulation of carbides and material weakening caused by the increase in holes. The method has been widely used because of its unique advantages and flexibility. Moreover, more and more studies have suggested that this method had a complete theoretical basis. Therefore, it is used to describe the creep curve characteristics and predict the creep life of high-temperature components. Specifically, the method can be described as a creep equation:

$$\varepsilon_c = \theta_1(1 - e^{-\theta_2 t}) + \theta_3(e^{\theta_4 t} - 1) \quad \text{(Eq 1)}$$

The four θ values are determined by the least-square regression analysis, and they are related to the temperature and stress. The coefficients θ_1 and θ_3 are the scaling parameters used to describe the decaying and accelerating of creep stages related to the strain. The coefficients θ_2 and θ_4 are the rate parameters which are used to characterize the curvatures of the decaying and accelerating of creep stages.

In addition, lg (θ_i) is concluded as the function of temperature and stress:

$$\lg \theta_i = a_i + b_i T + c_i \sigma + d_i T \sigma \quad \text{(Eq 2)}$$

where T is the temperature, i = 1, 2, 3, 4, and σ is the stress. lg(θ_i) linearly varies approximately with the functions of a stress and temperature. The parameters a_i, b_i, c_i and d_i can be obtained by using numerical calculation.

In this paper, the material and physical parameters for the creep constitutive equations which are presented under certain temperature conditions are calculated based on experimental data. If the creep equation and coefficient θ_i are defined on the basis of short-term tests at a high temperature, their values for long-term creep data can be predicted.

3. Materials and Creep Test

In accordance with ASTM E8M-04 (Ref 23), the test specimens with a gauge length of 100 mm and a diameter of 10 mm were fabricated from bars (as shown in Fig. 1), and the chemical composition of RPV material is 0.18% C, 0.23% Si, 1.40% Mn, 0.004% P, 0.13% Cr, 0.67% Ni and 0.48% Mo. Uniaxial creep tests were performed by using an INSTRON test machine in accordance with ASTME139 (Ref 24). The tested values were obtained from quantitative measurements for the specimens in the investigation. The loading ratio of lever arm was 20:1 with an accuracy of ±0.5%. The testing machine also provided displacement time diagram with an accuracy of ±0.0001 mm. The temperature of the furnace in the machine could reach up to 1,100 K with an accuracy of ±1 K.

During creep experiment, first, the specimens were heated to the test temperature at a heating rate of 5 K/min and were maintained for 0.5 h before loading. The load was applied and the successive measurements started once the designed experimental temperature was reached during each test. According to the creep displacement from the creep test machine, the total strain could be obtained. After the test, the samples were naturally cooled to environmental temperature in the furnace.

4. Experimental Results and Creep Curve

Generally, during the creep tests, the total strain (ε_{total}) can be divided into three different kinds of strains elastic strain ($\varepsilon_{elastic}$, loading stage), plastic strain ($\varepsilon_{plastic}$, loading stage) and creep strain (ε_{creep}, creep stage). Total strain could be obtained directly from the elongations recorded on the creep test machine. As soon as the temperature reached a constant value in each test, the loading and the successive measurements initiated. Subsequently, the actual amount of creep strains at each temperature and under different uniaxial loads was obtained according to Eq 3.

$$\varepsilon_{total} = \varepsilon_{creep} + \varepsilon_{elastic} + \varepsilon_{plastic} \quad \text{(Eq 3)}$$

4.1 Time-Independent Elastic-Plastic Curves

To obtain the actual $\varepsilon_{elastic}$ and $\varepsilon_{plastic}$, a set of elastic-plastic stress strain curves were obtained at different temperatures based on the tensile test data. The uniaxial time-independent elastic-plastic strain can be expressed as Eq 4, where E and σ_s represent the Young's modulus and yield stress, B and m are the temperature-dependent material constants, and σ_s can be easily obtained through uniaxial tensile tests at each temperature level.

$$\varepsilon = \frac{\sigma}{E} + \left(\frac{\sigma}{B}\right)^m \quad \text{(Eq 4)}$$

A least-square optimization scheme was used to provide the material constants B and m according to Eq 5.

$$error = \sum_{j=0}^{n} \left((\varepsilon_j^{\exp}) - (\varepsilon_j^{the})\right)^2 \quad \text{(Eq 5)}$$

ε^{the} and ε^{exp} are the theoretical and experimental strains, respectively. The theoretical strains were obtained based on Eq 4, whereas the experimental strains were obtained directly from the test measurements.

Table 1 lists the material constants B and m, which were obtained by minimizing the error function in Eq 5. Figure 2 shows the actual stress-strain curves of RPV material which were obtained through experimental tests at the temperature of 723, 823, 923 and 1023 K.

4.2 Time-Independent Plastic Creep Curves

Uniaxial creep tests were performed at 723 K under different stresses of 400, 385, 375 and 355 MPa, at 823 K under different stresses of 210, 190, 180 and 140 MPa, at 923 K under different stresses of 80, 70, 60 and 30 MPa, and at 1023 K under different stresses of 25 20, 15 and 10 MPa, respectively. During the creep tests, the temperature and load levels were constant and the variations of the total actual strain with time were obtained under various test conditions, including the initial loading strain ε_i and the time-independent plastic strain ε_t. In order to obtain pure creep strains ε_c, removal of the time-independent strains was necessary according to the data in Table 1, as shown Eq 6:

$$\varepsilon_c = \varepsilon_{total} - \varepsilon_i - \varepsilon_t \quad \text{(Eq 6)}$$

In order to separate the actual creep strains from the total actual strains, it is necessary to recognize the contributions of the time-independent plastic strain ε_t. The following equations are used to calculate ε_t

$$\sigma_{t+\Delta t} = F/A_t(1 + l/l_t)$$

$$\Delta\varepsilon_t = (\sigma_{t+\Delta t}/B)^m - (\sigma_t/B)^m \quad \text{(Eq 7)}$$

where σ_t and $\sigma_{t+\Delta t}$ are the actual stress at time t and $t + \Delta t$, respectively. A_t and $A_{t+\Delta t}$ are the actual cross sections of the specimen at time t and $t + \Delta t$, respectively. l_t and Δl are the gauge length at time t and the time interval Δt.

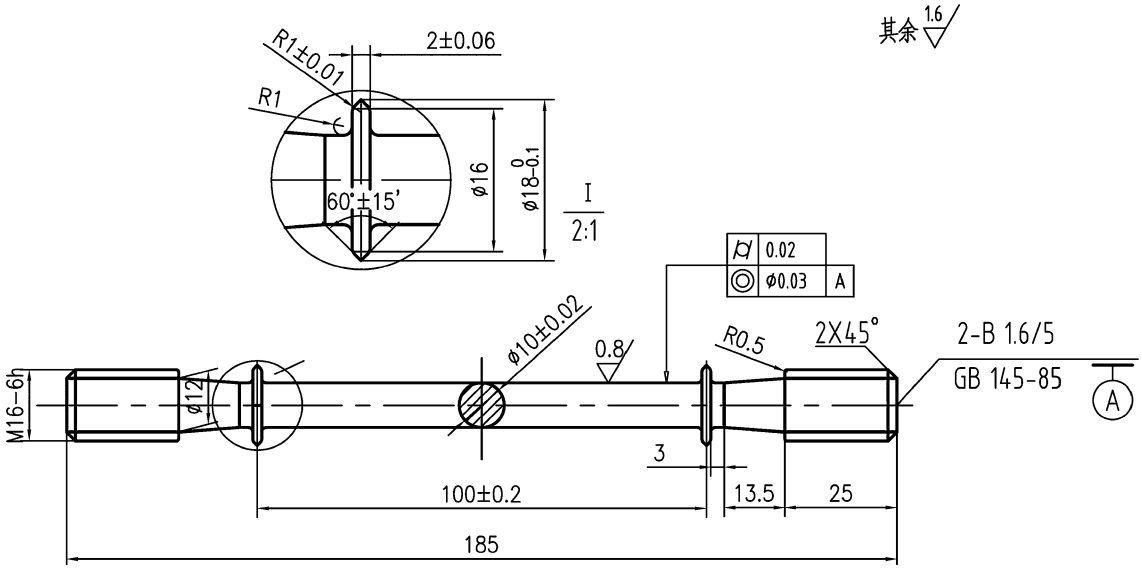

Fig. 1 Standard creep specimen (unit: mm)

Table 1 Elastic-plastic properties of RPV material obtained by experiments at different temperature levels

Temperature, K	Elastic module, MPa	Yield stress, MPa	*B*, MPa	*m*
723	1.58×10^5	345	515.33	15.19
823	1.44×10^5	298	403.24	20.61
923	1.15×10^5	142	191.33	14.06
1023	0.70×10^5	55	81.94	14.57

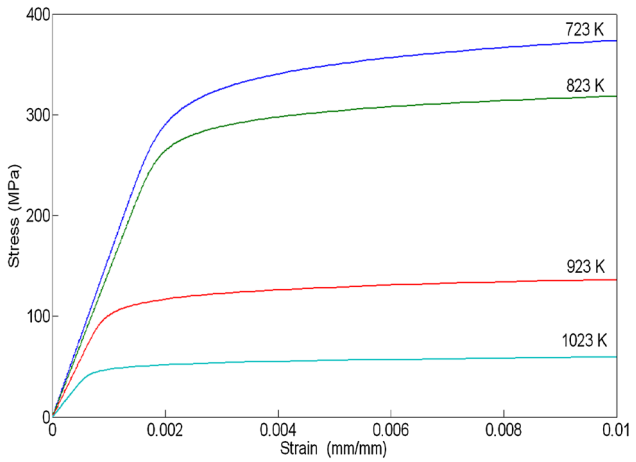

Fig. 2 Stress-strain curves of RPV material obtained from experiments at different test temperatures

However, the applied stress load quickly increased from zero to the designed value and it is significantly lower than the yield stress when the temperature was 823, 923 and 1023 K during the creep tests. Therefore, the time-independent plastic straining ε_t was zero. In that way, the creep Eq 1 can be expressed as:

$$\varepsilon_c = \varepsilon - \varepsilon_i = \theta_1\left(1 - e^{-\theta_2 t}\right) + \theta_3\left(e^{\theta_4 t} - 1\right) \quad \text{(Eq 8)}$$

4.3 Creep Curves and Equation

The creep test data would usually have a large scatter due to the nonlinear behavior of the creep deformation. In addition, errors exist in the data recording and discrepancies occur in test results in each test. Therefore, the most appropriate constitutive parameters for all test data should be obtained through numerical methods. So, the optimization techniques are applied to estimate procedure for constitutive parameters of creep tests, and ensure that the mode should be more suitable for the experimental data. For this purpose, different optimization techniques can be used, among which the least-square method is the most viable. By using this method, constitutive parameters can be obtained through minimizing the difference between the values of the experimental data points and the calculated amount. The optimization techniques can be defined as:

$$\text{error} = \sum\nolimits_{i=1}^{n} \left(\left(\varepsilon_i^{\text{exp}}\right) - \left(\varepsilon_i^{\text{the}}\right)\right)^2 \quad \text{(Eq 9)}$$

The theoretical values were obtained according to Eq 8 at different stress and temperature levels in each test. The experimental values and fitting curves are shown in Fig. 3, 4, 5 and 6. Based on the nonlinear optimization method, the constitutive parameters θ_1, θ_2, θ_3 and θ_4 can be obtained in accordance with Eq 9. Table 2 presents the calculated constitutive parameters of constitutive equations. Moreover, the correlation value R^2 is more than 99.61%. That means the θ method has a good relevance with the actual test data.

5. Results and Discussion

5.1 Modeling of Relationship Between T, h and r

Each lg(θ_i) value can be defined as the function of stress and temperature, and their relationship can be described according to Eq 2. Value of θ can be known at 723, 823, 923 and 1023 K according to Table 2. A kind of commercially available software (OriginPro 8) has been used to obtain the values of coefficients a_i, b_i, c_i and d_i by least-square method. The units of time, temperature and stress are hour (h), degree K (T) and stress (MPa), respectively. Table 3 presents the coefficients a_i, b_i, c_i and d_i. The relationships and coefficients indicate that Eq 2 can permit both an interpolation and an extrapolation of the creep data and the short-term test results can be used to predict the long-term creep curves.

In present study, the other θ_i can be obtained based on parameters a_i, b_i, c_i and d_i according to Eq 2 at designed or specified temperature and stress. Moreover, creep equation can be expressed for other stress conditions based on θ value. Therefore, the formulas can be used to obtain creep equation of RPV material at any temperature and any stress value and can be applied to explore the creep performance at different temperatures for nuclear power equipment and be used as a reference for design and safety assessment.

5.2 Minimum Creep Strain Rate

Creep is divided into three stages, including decaying creep, steady-state creep and accelerating creep. Normally, minimum creep strain rate can be described as the steady-state creep rate. It is an important parameter that is used to represent the characterization of creep resistance. The creep rate is usually used as an important parameter to predict the creep life of high-temperature materials. The creep rate can be determined by differentiating Eq 1 with respect to the time:

$$\varepsilon' = \frac{d\varepsilon}{dt} = \theta_1\theta_2 e^{-\theta_2 t} + \theta_3\theta_4 e^{\theta_4 t} \quad \text{(Eq 10)}$$

Depending on differentiating Eq 10, the second and the third time differentiations of strain ε'' and ε''' can be described as:

$$\varepsilon'' = \frac{\mathrm{d}^2\varepsilon}{\mathrm{d}t^2} = -\theta_1(\theta_2)^2 e^{-\theta_2 t} + \theta_3(\theta_4)^2 e^{\theta_4 t} \quad \text{(Eq 11)}$$

$$\varepsilon''' = \frac{d^3\varepsilon}{dt^3} = \theta_1(\theta_2)^3 e^{-\theta_2 t} + \theta_3(\theta_4)^3 e^{\theta_4 t} \quad \text{(Eq 12)}$$

Since θ_i are positive, as given in Eq 10, $\mathrm{d}\varepsilon/\mathrm{d}t$ is nonnegative. Thus, ε is an increasing function of time t as the definition of creep. It is assumed that $\mathrm{d}\varepsilon^2/\mathrm{d}t^2 = 0$, a minimum creep rate point can be known. Moreover, it is the only inflection point since $\mathrm{d}^3\varepsilon/\mathrm{d}t^3$ is not zero or positive at this point. Thus, the time at a minimum creep rate t_m can be obtained by differentiating Eq 10 when $\mathrm{d}\varepsilon^2/\mathrm{d}t^2=0$ and can be calculated according to:

$$t_m = \frac{1}{\theta_2 + \theta_4} \ln \frac{\theta_1(\theta_2)^2}{\theta_3(\theta_4)^2} \quad \text{(Eq 13)}$$

Table 4 shows the results. The data of minimum creep strain rate indicate that the minimum creep strain rate gradually decreases with the increase in stress.

The estimated exponent (n) in the Norton relationship was obtained to gain some insight into the possible creep deforma-

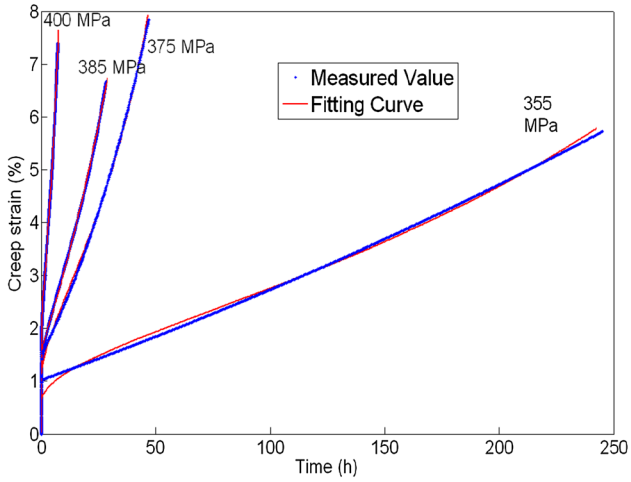

Fig. 3 Experimental and fitted creep curves at 723 K

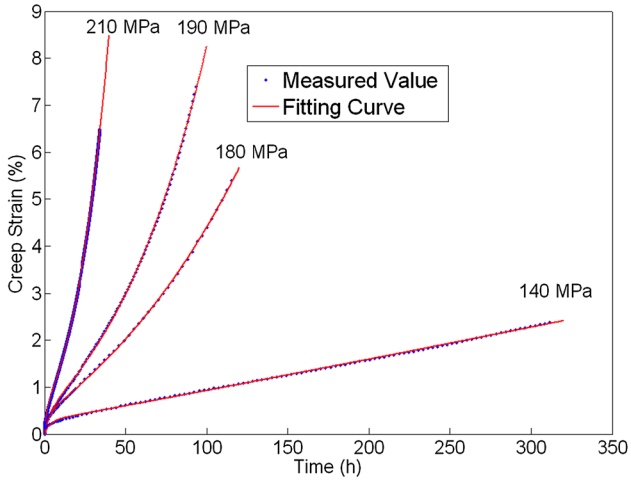

Fig. 4 Experimental and fitted creep curves at 823 K

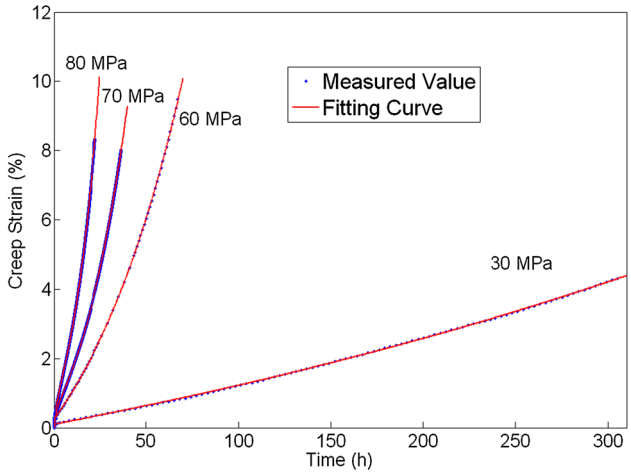

Fig. 5 Experimental and fitted creep curves at 923 K

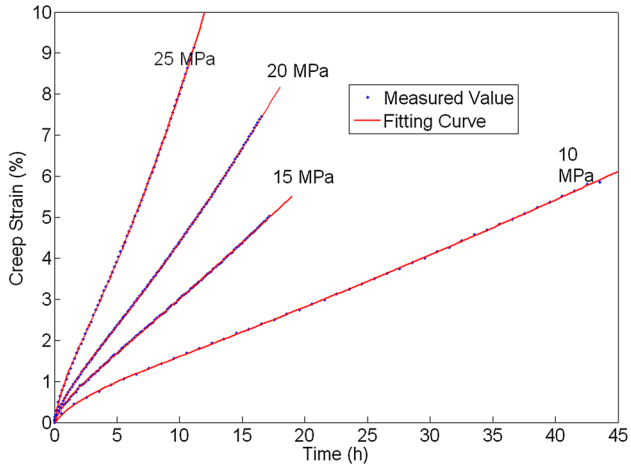

Fig. 6 Experimental and fitted creep curves at 1023 K

tion mechanism. Namely, the creep constants for Norton's power law can be described as the following equation:

$$\dot{\varepsilon} = A\sigma^n \quad \text{(Eq 14)}$$

"A" is the rate parameters, and n is the creep index for the creep curve. The coefficient n reflects the effect of different stresses and creep mechanism at the same temperature.

By adopting optimization technique and based on the results, the creep constants for Norton's power law, "A" and "n" could be obtained for the RPV material steel in Table 5. The creep index n is corresponding to the slope of straight line in Fig. 7. The intercept of straight line is the logarithm value lg (A) of the speed coefficient of creep for the RPV material at 723, 823, 923 and 1023 K. The relationship between the minimum creep rate and the stress revealed a good linearity. The values of the minimum creep rates were determined by a minimum value at the inflection point of the creep curve. Then,

Table 2 Creep parameters θ_1, θ_2, θ_3, θ_4 at different test conditions

T (K)	Stress, MPa	θ_1	θ_2	θ_3	θ_4	R^2, %
723	400	2.24	6.55	4.24	1.08E−1	99.61
723	385	1.60	6.74	7.31	1.83E−2	99.76
723	375	1.50	6.38	4.73	1.80E−2	99.84
723	355	1.02	6.11	10.50	1.51E−3	99.78
823	210	5.19E−1	7.14E−1	1.86	4.16E−2	99.97
823	190	5.20E−1	2.19E−1	2.11	1.54E−2	99.97
823	180	4.22E−1	3.52E−1	3.19	8.11E−3	99.94
823	140	2.76E−1	2.94E−1	26.68	2.41E−4	99.91
923	80	6.49E−1	6.52E−1	2.80	5.90E−2	99.99
923	70	4.46E−1	7.69E−1	3.17	3.33E−2	99.99
923	60	2.46E−1	5.39	4.36	1.68E−2	100.00
923	30	9.65E−2	7.38	5.57	1.84E−3	99.99
1023	25	6.57E−1	1.64	12.52	4.64E−2	99.99
1023	20	5.23E−1	9.94E−1	16.01	2.71E−2	99.99
1023	15	3.90E−1	1.10	45.31	5.64E−3	99.99
1023	10	4.67E−1	4.85E−1	21.40	5.20E−3	99.99

Table 3 Coefficients a, b, c and d

Parameter	a	b	c	d	R^2, %
lg(θ_1)	−7.286	6.662E−3	−1.369E−3	1.154E−5	95.51
lg(θ_2)	4.583	−4.008E−3	4.132E−2	−6.048E−5	77.81
lg(θ_3)	1.803	−3.603E−4	2.710E−2	−4.010E−5	73.21
lg(θ_4)	−21.576	1.8917E−2	−2.979E−2	6.416E−5	74.31

Table 4 Minimum creep rate at various temperatures and stress levels

723 K		823 K		923 K		1023 K	
Stress (MP)	ε'_{Min}	Stress, MP	ε'_{Min}	Stress, MP	ε'_{Min}	Stress, MP	ε'_{Min}
400	5.26E−1	210	1.04E−1	80	2.38E−1	25	6.70E−1
385	1.38E−1	190	4.50E−2	70	1.32E−1	20	4.93E−1
375	8.79E−2	180	1.43E−2	60	7.56E−2	15	2.65E−1
355	1.58E−2	140	6.46E−3	30	1.03E−2	10	1.19E−1

Table 5 n and A values from Norton's power law

Parameter	723 K	823 K	923 K	1023 K
n	27.75	7.08	3.12	1.93
A	7.90E−76	3.66E−18	2.47E−7	1.43E−3

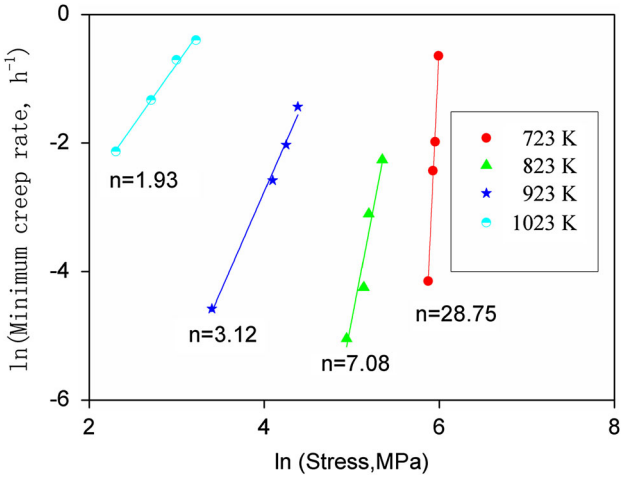

Fig. 7 Stress dependence of the minimum creep rate at 723, 823, 923 and 1023 K

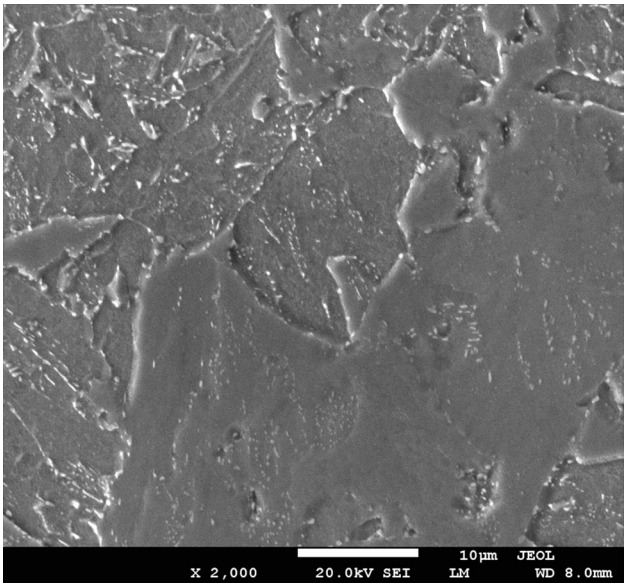

Fig. 8 SEM image of a typical microstructure of sample after 116 h creep at 823 K and 180 MPa

it could be used to calculate the minimum creep rate under the condition of low stress based on parameter A and n.

5.3 Creep Damage Mechanism of RPV Material

After high-temperature creep test, specimen in the middle part of the cross section of the interception of samples for grinding and polishing, with 4 vol.% picric acid, 4 vol.%HNO_3 and 92 vol.% C_2H_5OH corrosive reagent, cleaning and drying, the microstructure observation was performed by scanning electron microscope (SEM). After high-temperature creep test,

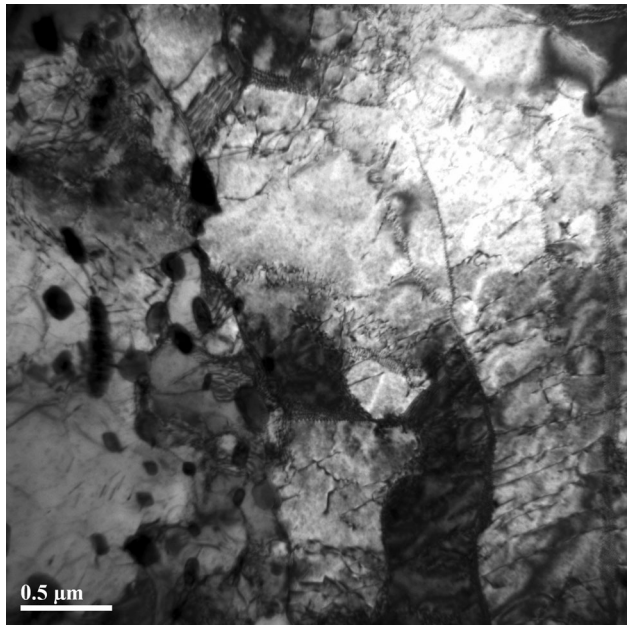

Fig. 9 TEM image of a typical microstructure of sample after 116 h creep at 823 K and 180 MPa

the cross section of SEM specimen is 0.3 mm thick sheet by line cutting, and mechanical grinding to about 100 μm. Mechanical punching machine can be used to obtain wafer with diameter of 3 mm, and worn thin to about 40 μm. Finally, it is placed in the disk with samples of platinum wire clip into the twin-jet electropolishing thinning until perforation. The electrolyte consists of 5 vol.% $HClO_4$ and 95 vol.% C_2H_5OH cooled by liquid nitrogen. Then, observation of the thin foil was carried out by the transmission electron microscope (TEM).

Figure 8 shows SEM image of a typical microstructure of sample, and Fig. 9 shows TEM image of a typical microstructure of sample. The SEM observation shows that microstructure of RPV material at 550 °C under different stresses after creep test remains the bainite morphology, which is similar to the microstructure obtained in the heat-treated conditions. The distribution of carbides is basically same. The TEM observation shows that, compared to the original heat-treated condition, the dislocation density in the lath-like bainite of RPV material at 550 °C under different stresses after creep tests changes significantly. The lath-like bainites still maintain high dislocation density under the high-stress condition, but the dislocation mainly formed two-dimensional dislocation network. The above fact shows that the creep is a process of the coexistence of dislocation slip and dynamic recovery in the high-stress condition, in which the dynamic recovery was determined by the dislocation climb. Under the condition of low stresses, the internal dislocation density in the lath-like bainites is relatively low, mainly forming two-dimensional dislocation network or small-angle sub-grain boundaries. The fact shows that the long-

Table 6 Details of the creep tests involving stress vs. time at ε = 1%

723 K		823 K		923 K		1023 K	
Stress, MP	$t_{\varepsilon=1\%}$, h	Stress, MP	$t_{\varepsilon=1\%}$, h	Stress, MP	$t_{\varepsilon=1\%}$, h	Stress, MP	$t_{\varepsilon=1\%}$, h
400	0.09	210	5.88	80	2.77	25	0.95
385	0.09	180	14.78	70	5.17	20	1.67
375	0.10	170	20.65	60	9.63	15	2.55
355	6.01	140	108.78	30	83.16	10	5.35

Table 7 Details of the creep tests involving stress vs. time at ε = 3%

723 K		823 K		923 K		1023 K	
Stress, MP	$t_{\varepsilon=3\%}$, h	Stress, MP	$t_{\varepsilon=3\%}$, h	Stress, MP	$t_{\varepsilon=3\%}$, h	Stress, MP	$t_{\varepsilon=3\%}$, h
400	1.52	210	20.36	80	10.23	25	3.7
385	9.17	180	50.28	70	17.66	20	6.55
375	14.33	170	73.15	60	29.13	15	10
355	114.58	140	386.78	30	227.16	10	22.05

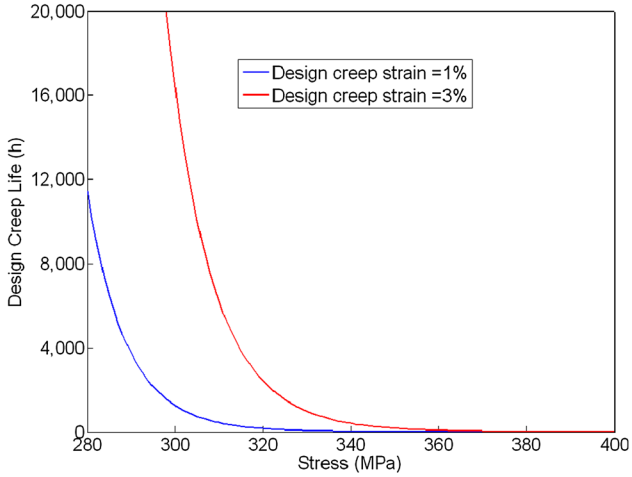

Fig. 10 Stress vs. design creep life curve at 723 K

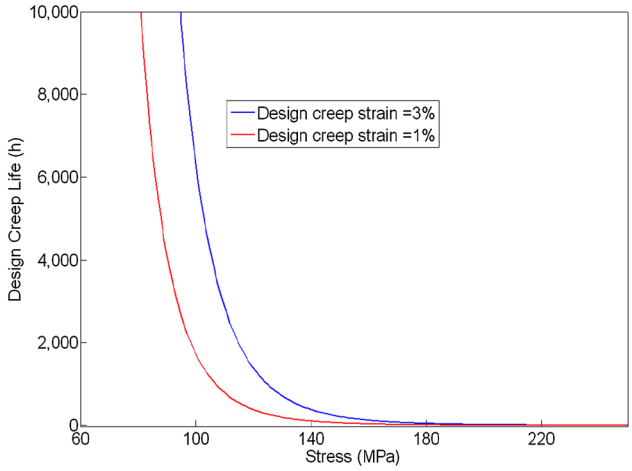

Fig. 11 Stress vs. design creep life curve at 823 K

term creep should mainly belong to a dislocation dynamic recovery process, which was determined by the climbing of dislocation.

In addition, the RPV material has different structures under diverse creep temperatures, which makes it have different high-temperature creep mechanical properties. Accordingly, the creep damage mechanism can also be different. According to the creep theory of metallic materials, the creep stress exponent of RPV material at 827 K with bainite microstructure arrives at 7.08, see Table 5. During the high-temperature creep test, the climbing mechanism of dislocation coupled with dynamic recovery of dislocations and interaction mechanism between the dislocation and carbide particles.

5.4 Prediction of Time Reaching a Limiting Strain

Once the shape of the creep curve is acquired through a mathematical expression by using Eq 1, the time reaching any creep strain can be calculated. The time reaching a limiting strain is important from a design viewpoint. For instance, ASME nuclear Code NH requires information about the time when 1 and 3% strains were produced for a design of time-dependent materials (Ref 19). For this reason, it will be necessary to describe the shape of the long-term creep curves at various stresses and temperatures. The time reaching any creep strain (ε^{tr}) under the condition of any stress and temperature can be obtained easily by solving the following Eq 1 numerically:

$$\theta_1\left(1-e^{-\theta_2 t_r}\right)+\theta_3\left(e^{\theta_4 t_r}-1\right)-\varepsilon^{t_r}=0 \qquad \text{(Eq 15)}$$

where ε^t is the creep strain at any specified value required for a design purpose.

The time is acquired when ε = 1% at 723, 823, 923 and 1023 K under different stress conditions by creep test, see Table 6. When ε = 3%, the corresponding time could be acquired, see Table 7. Both stress and design creep lift curve could be acquired according to Eq 15 from stress-time data under given strain conditions.

Figure 10, 11 12 and 13 show the creep strain values for SA508 which were calculated under the condition of temperature 723, 823, 923 and 1023 K. Also, this figure shows the corresponding time when the creep strains reach 1% and 3% under different stress conditions at 723, 823, 923 and 1023 K. Moreover, the curve can be obtained for the designed stress values at different time.

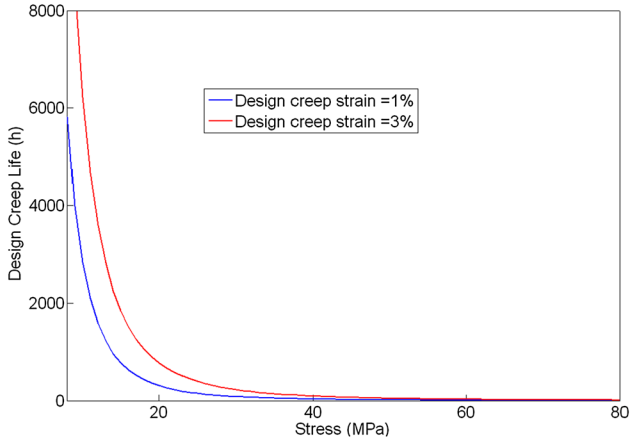

Fig. 12 Stress vs. design creep life curve at 923 K

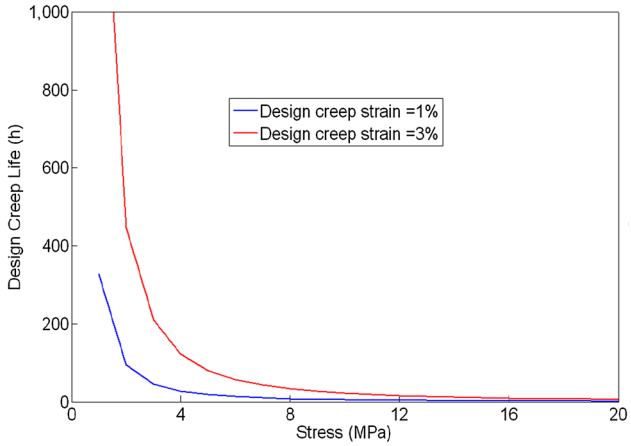

Fig. 13 Stress vs. design creep life curve at 1023 K

It is contended that the t_r estimates reported here have direct design usefulness because they are derived from tensile creep test data. It is known that, in elevated-temperature service, RPV material steel is subject to tensile stress. However, it should be noted that these estimates would be affected by a number of variables, among which the most significant factor is the quickly changed temperature between the started operation and extremes accidents. This stress and designed creep life curve can be used as a reference for design and safety assessment for nuclear power equipment.

6. Conclusion

The creep experimental data can be obtained under different stresses at 723, 823, 923 and 1023 K. The θ projection constitutive model is obtained through a creep experiment and can be used to describe the high-temperature creep behavior of RPV material. Based on the nonlinear optimization method, the constitutive parameters θ_1, θ_2, θ_3 and θ_4 can be obtained, and the correlation value R^2 is more than 99.61%. Thus, the θ method has a good relevance with the actual test data. The time when the rupture strain reaches 1 and 3% can be predicted, and the creep extrapolation techniques can be assessed using parameters θ. As a result, the typically minimum creep rate can be obtained under different stresses for RPV material.

The coefficients a_i, b_i, c_i and d_i can be calculated based on the θ data. The short-term test results could be used to predict the long-term creep curves and creep equation of RPV material at any temperature and any stress value. Moreover, these conclusions and equations can be employed to explore the creep performance at different temperatures for nuclear power equipment and used as a reference for design and safety assessment.

References

1. A. Baldan and E. Tascioglu, Assessment of θ-Projection Concept and Fracture Cavitation, *J. Mater. Sci.*, 2008, **43**, p 4592–4606
2. N. Haghdadi, A. Zarei-Hanzaki, and H.R. Abedi, The Flow Behavior Modeling of Cast A356 Aluminum Alloy at Elevated Temperatures Considering the Effect of Strain, *Mater. Sci. Eng. A*, 2012, **535**, p 252–257
3. Y.C. Lin, Y.C. Xia, M.S. Chen, Y.Q. Jiang, and L.T. Li, Modeling the Creep Behavior of 2024-T3 Al Alloy, *Comput. Mater. Sci.*, 2013, **67**, p 243–248
4. Y.Q. Jiang, Y.C. Lin, C. Phaniraj, Y.C. Xia, and H.M. Zhou, Creep and Creep–Rupture Behavior of 2124-T851 Aluminum Alloy, *High Temp. Mat. Pr-isr.*, 2013, **32**, p p533–p540
5. P.W. Davies, W.J. Evans, K.R. Williams, and B. Wilshire, An Equation to Represent Strain Time Relationship During High Temperature Creep, *Scr. Metall.*, 1969, **9**, p 671–674
6. L.D. Blackburn, Isochronous stress–strain curves for austenitic steels, *The Generation of Isochronous Stress–Strain Curves*, G.V. Smith, Ed., ASME, NewYork, 1972,
7. R.W. Evans, J.D. Parker, and B. Wilshire, The Theta Projection Concept a Model-Based Approach to Design and Life Extension of Engineering Plant, *Int. J. Pres. Vessels Pip.*, 1992, **50**, p 147–160
8. F. Garofalo, *Fundamentals of Creep and Creep Rupture in Metals*, Macmillan Co, New York, 1969
9. K. Maruyama, C. Harada, and H. Oikawa, A Strain–Time Equation Applicable Up to Tertiary Creep Stage, *J. Soc. Mater. Sci. Jpn.*, 1985, **34**, p 1289–1295
10. C. Phaniraj, B.K. Choudhary, B. Raj, and T. Jayakumar, Comment on "Deformation and Damage Processes During Creep of Incoloy MA957" by B. Wilshire and T.D. Lie', *Mater. Sci. Eng. A*, 2005, **398**, p 373–375
11. B. Wilshire and D.R.J. Owen, *Recent Advances in Creep and Fracture of Engineering Materials and Structures*, Pineridge Press, Swansea, 1982
12. W. Blum and B. Reppich, *Creep Behavior of Crystalline Olids*, Pineridge Press, Swansea, 1985
13. H. Wolf, M.D. Mathew, S.L. Mannan, and P. Rodriguez, Prediction of Creep Parameters of Type 316 Stainless Steel Under Service Conditions Using the h-Projection Concept, *Mater. Sci. Eng. A*, 1992, **159**, p 199–204
14. S. Fujibayashi, M. Miura, and K. Togashi, Life Prediction of Low Alloy Ferritic Steels Based Upon the Tertiary Creep Behavior, *ISIJ Int.*, 2004, **44**, p 919–926
15. C.M. Omprakash, A. Kummar, B. Srivathsa, and D.V.V. Satyanarayana, Prediction of Creep Curves of High Temperature Alloy using θ-Projection Concept, *Proc. Eng.*, 2013, **55**, p 756–759
16. Y.C. Lin, Y.C. Xia, X.S. Ma, Y.Q. Jiang, and M.S. Chen, High-Temperature Creep Behavior of Al-Cu-Mg Alloy, *Mater. Sci. Eng. A.*, 2012, **550**, p 125–130
17. Y.C. Lin, Y.Q. Jiang, H.M. Zhou, and G. Liu, A New Creep Constitutive Model for 7075 Aluminium Alloy Under Elevated Temperatures, *J. Mater. Eng. Perform.*, 2014, **23**, p 4350–4357
18. B. Wilshire and H. Burt, creep Data Prediction for Aluminium Airframe Alloys, *Mater. Sci. Forum*, 2003, **464**, p 261–266
19. Woo-Gon Kim, Song-Nan Yin, Yong-Wan Kim, and Jong-Hwa Chan, Creep Characterization of a Ni-Based Hastelloy-X Alloy by Using Theta Projection Method, *Eng. Fract. Mec.*, 2008, **75**, p 4985–4995
20. B.F. Dyson, D.R. Hayhurst, and J. Lin, The Ridged Uniaxial Testpiece Creep and Fracture Predictions Using Large-Displacement

Finite-Element Analyses, *Proc. R. Soc. Lond. Ser. A*, 1996, **452**, p 655–676
21. B. Jiang, T. Wang, Z. Qua, R. Wu, and M. Zhang, Creep Behaviors of Mg-5Li-3Al-(0,1)Ca Alloys, *Mater. Des.*, 2011, **34**, p 863–866
22. F.V. Tahami, A.H. Daei-Sorkhabi, and F.R. Biglari, Creep Constitutive Equations for Cold-Drawn 304l Stainless Steel, *Mater. Sci. Eng. A*, 2010, **27**, p 4993–4999
23. ASTM, E8M-04: Standard Test Methods for Tension Testing of Metallic Materials (Metric), *Annual Book of ASTM Standards*, ASTM International, West Conshohocken, PA, 2004
24. ASTM, E139e06: Standard Tests of Metallic Materials, Creep, Creep-rupture and Stress Rupture Tests of Metallic Materials, *Annual Book of ASTM Standards*, ASTM International, West Conshohocken, PA, 2006